Journal of Sound and Vibration (2000) **231**(3), 611–617
doi:10.1006/jsvi.1999.2548, available online at http://www.idealibrary.com on IDEAL®

ACOUSTIC NOISE SOURCE MODELLING BASED ON MICROPHONE ARRAY MEASUREMENTS

S. BRÜHL AND A. RÖDER
DaimlerChrysler AG, Postfach 80 04 65, *D*-81 663 *München, Germany*

(*Received in final form* 23 *September* 1999)

A method will be presented which allows a construction of an acoustic source model based on the analysis of microphone array measurements during a train pass-by. The conventional array beam-forming technique is used as a kind of pre-processing or first order analysis to calculate in a second step the true source strengths by a back-projection method. The final equation to be solved connects the source power distribution on the vehicle surface with the measured microphone array amplitudes via a Green's function transfer matrix. By these means the side-lobe effects of the array characteristics as well as the Doppler frequency shift and amplitude augmentation of the sources are removed. The model is updated for consecutive time slices during the pass-by so that it is possible to study directional and time-dependent effects on the source characteristics. The method has been applied to measurements on the ICE-V train where three known artificial noise sources (loudspeakers) had been mounted on the outside of the sidewall. The source power distribution function gives a much better source separation than the conventional beam-forming result. The calculated source strengths show a good agreement with the true values.

1. INTRODUCTION

Microphone arrays are a well-known tool to localize sound sources and have been applied with success on high-speed trains such as ICE, TGV and the magnetic train Transrapid [1, 2]. The output of the conventional array measurement analysis software (AMAS), however, still yields immission levels which are calculated for the position of the array center. Moreover, the result is influenced by the beam-forming method and the ability to localize and separate different sources depends on the frequency range and the microphone geometry which has been used; the main beamwidth and the side-lobes lead to a broadening of the source area and to an overestimate of the local source powers.

In order to overcome and remove these influences, a source density modellization approach (SDM) is described which allows an improvement of the (first order) AMAS data to obtain true and objective source power data. A model of a point source distribution will be constructed used to simulate the beam-forming analysis of the AMAS software. The desired source amplitudes are then obtained by the fit of the model simulation to the actual AMAS measurement results.

0022-460X/00/130611 + 07 $35.00/0

2. THEORETICAL FORMULATION

The well-known beam-forming of an arrangement of microphones with regard to a chosen focus point x_0 is carried out using a linear superposition of the delayed individual microphone signals p_j:

$$a_{(k)}(\vec{x}_0, t) = \sum_{j=1}^{N} w_j^{(k)} \cdot p_j(t + (r_j(\vec{x}_0)/c)) \tag{1}$$

where $w_j^{(k)}$ is a set of arbitrary weighting factors with the normalization condition $\sum_{j=1}^{N} w_j^{(k)} = 1$. The individual time delays are governed by the distance vector $r_j(x_0)$ between microphone j and the desired focus point x_0. Assuming an uncorrelated discrete source distribution with spherical radiation characteristics it is possible to derive a matrix equation which connects the source power density vector $\Psi_m(q_m; \omega')$ as a function of the source position q_m with the power spectral array amplitude vector $A_n^{kk'}(\omega) = |a_k^*(x_n; \omega) \cdot a_{k'}(x_n; \omega)|$ as a function of the focus co-ordinate x_n [3, 4]:

$$A_n^{kk'}(\omega) = \sum_{m, \omega'} H_{nm}^{kk'}(\omega, \omega') \cdot \Psi_m(\omega'). \tag{2}$$

The projection matrix **H** includes the superposition of the basic transfer Green's functions between the individual source and receiver points according to the beam-forming of Equation (1) and thus contains all the phase information connecting the array geometry with the source geometry. Furthermore, for moving sources with high velocities a frequency coupling due to the Doppler effect will arise in Equation (2). This coupling occurs only for off-diagonal matrix elements of **H** where the focus co-ordinate x_n does not coincide with the source co-ordinate q_m. An approximate approach leads to the formula (cf. Figure 1)

$$\omega_1 = \omega_0 \frac{1 - M \cos\theta_j(x_0)}{1 - M \cos\theta_j(q_0)} \tag{3}$$

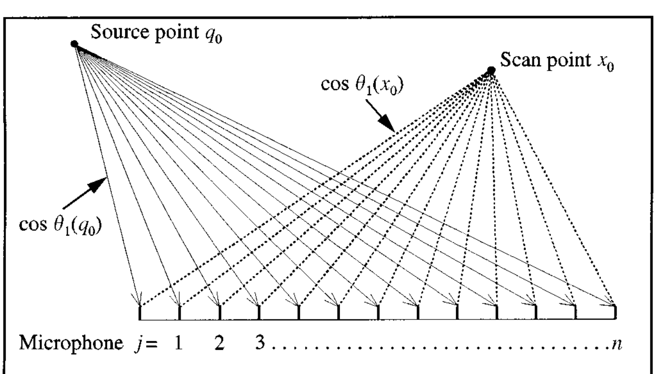

Figure 1. Doppler effect of source at q_0 while the array is focused to scan point x_0.

for the individual microphone positions j (Figure 1). $M = v/c$ is the Mach number. Equation (2) is a general formulation where two different weighting sets k and k' can be used to couple different subarrays of the total microphone arrangement (e.g., horizontal and vertical parts of a cross-array). In the case of a line or planar array configuration only one weighing set is used ($k = k'$). By an inversion of equation (2) it is now possible to calculate the desired source power values $\Psi_m(\omega)$. The advantage of this approach is to use the AMAS result as a pre-processed data set which already contains reliable localization information. Thus, it is possible to define the model in a highly efficient way with respect to the number of sources and the spatial resolution and arrangement. However, in order to demonstrate clearly the capabilities of the method, the following investigations have been conducted without the use of any *a priori* information about the true position of the sources. In all cases, an equidistant source distribution (about 200 sources with 20 cm spacing) has been used to cover the total area of the first order AMAS result.

3. COMPUTER SIMULATIONS [4]

To perform computer simulations a program module is first used which creates single microphone signals to simulate real measurement data for a given situation of moving sources. In a second step, these data are then used for the AMAS and SDM analysis. Figure 2 shows the result of a simulation for a single static source located at $x = -2$ m to the left of the array centre. The source is assumed to exhibit ideal omnidirectional radiation characteristics emitting a frequency of 818 Hz with a source power of 126 dB re pW. For this test the array design and the source position have been chosen in a way that aliasing problems occur (see broad shoulder for $x > 4$ m). The left-hand diagram shows the AMAS immission result (measurement) and the model fit. The right-hand diagram shows the resulting source distribution (solution of equation (2)) which leads to the fit. All the side-lobe and aliasing effects have been removed and only a single point source at the desired position remains.

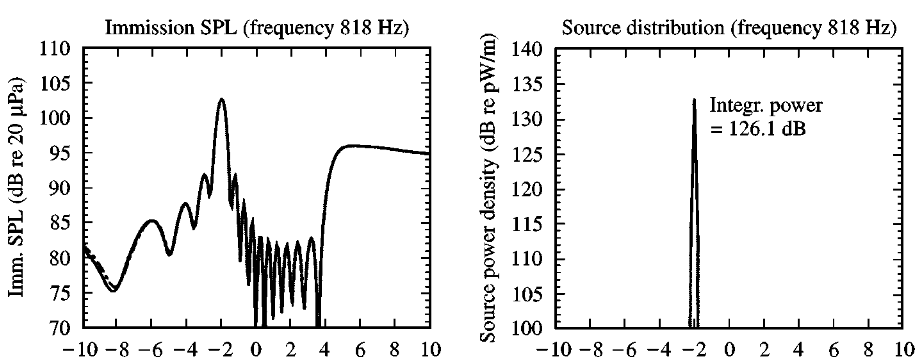

Figure 2. Simulation of a single static source. Left: AMAS result (full line) and SDM fit (dotted). Right: source distribution.

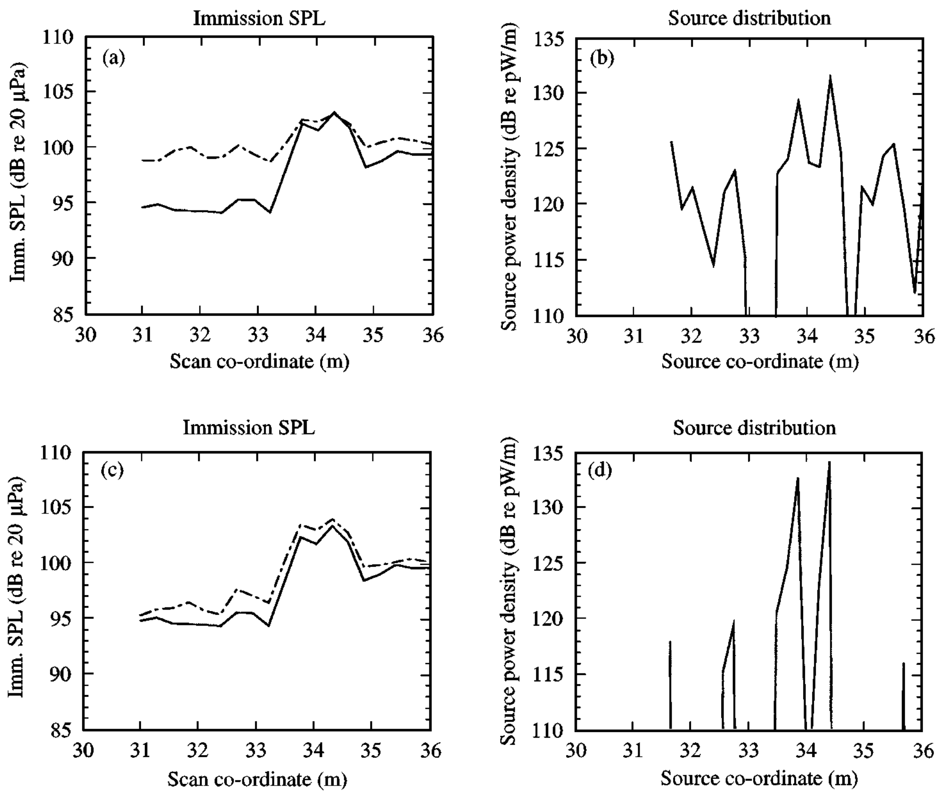

Figure 3. Simulation for two moving sources with velocity 280 km/h: (a, b) SDM calculation without frequency coupling, (c, d) SDM calculation with frequency counting. ——, measurement; – – – –, single and multiple frequency fit.

In Figure 3 the results of a simulation are shown, where two very close sources ($\Delta x = 55$ cm) are passing the array with 280 km/h. Again ideal omnidirectional monochromatic sources have been assumed, emitting frequencies of 820 and 990 Hz respectively. A cross array was used with an additive beam-forming of all microphones, but only a horizontal cut of the 2-D results is shown. The modellization has been done for a time slice, when the two sources are in front of the array and the Doppler effect has the most significant influence. In the upper pair of diagram (a, b), the SDM calculation was done without the frequency coupling of equation (3). The SDM fit to the measurement (AMAS) data is poor in the regions where no real sources are present. The source distribution (Figure 3(b)) shows large areas with false source amplitudes. On the other hand, the improved treatment with the frequency coupling leads to a satisfactory fit result (Figures 3(c), and (d)). The two sources are detected clearly and the false source amplitudes are suppressed by a least 14 dB. Because of the poor directional characteristics of the additive cross array, the off-diagonal elements of the projection matrix **H** play an important role, and therefore the frequency coupling cannot be neglected in the present case. In the case of an array configuration with a very strong main beam (e.g., planar array) the frequency coupling will be less important and may be neglected in a crude approach.

4. MEASUREMENTS ON ICE-V

To verify the modellization method with real measurement data a test study was carried out with three adjustable sound sources (loudspeakers) mounted in the window section of the ICE-V (see Figure 4). A cross-array with 2×12 microphones (spacing 30 cm) was used. Details about the experimental set-up are given in references [5, 6]. The measurements were made at different train speeds and different configurations of active sources. The loudspeakers were driven independently with different single frequencies (590/820/990 Hz). To calibrate the source power of the loudspeakers the train was stopped in front of the array and each individual source was measured at rest. The analysis was made for the whole pass-by history of subsequent time slices as shown in Figure 5. The AMAS and SDM calculations were performed with two different beam-forming algorithms: (a) multiplicative coupling of horizontal and vertical subarrays (i.e, $k \neq k'$ in equation (2)), and (b) simple additive superposition of all 24 microphones (only one weighting set $k = k'$ in equation (2)). The results of the two methods are shown in Figure 6 as 2-D image plots. The situation has been taken for the time slice when the loudspeakers were opposite to the array position. Horizontal co-ordinates are measured with reference to the head of the power car. For the SDM result no graphical interpolation has been used in order to indicate the cell size of the sources. The localization of the three loudspeakers comes out perfectly and in particular the source in the middle is separated clearly. In the source distribution for the multiplicative method the side-lobe background cannot be removed totally. This is improved by use of the additive method, although the beam-forming characteristics in this case is poorer than for the multiplicative method.

By integrating over the relevant source areas it is possible to calculate the total power level of the individual sources. This has been done for the whole time history of the pass-by. The chosen integration area was $0{\cdot}6 \times 0{\cdot}6\ \mathrm{m}^2$. (*The decision on how to define the integration area is up to the user and should depend on the actual source*

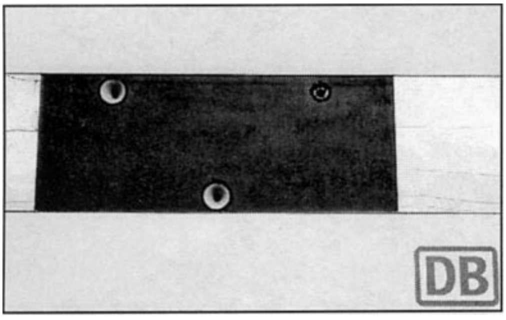

Figure 4. Window section of ICE-V passenger car with mounted loudspeakers.

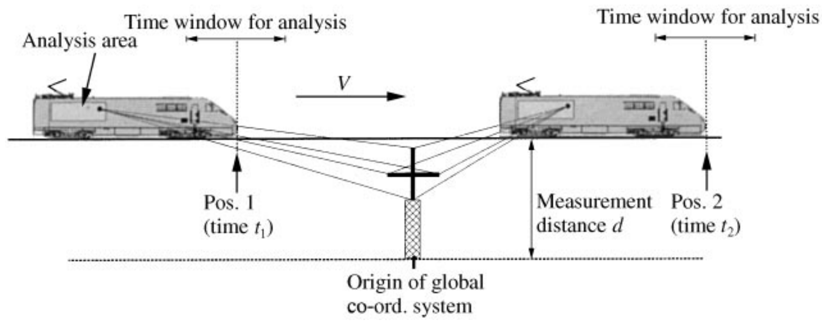

Figure 5. Analysis of different time slices during pass-by.

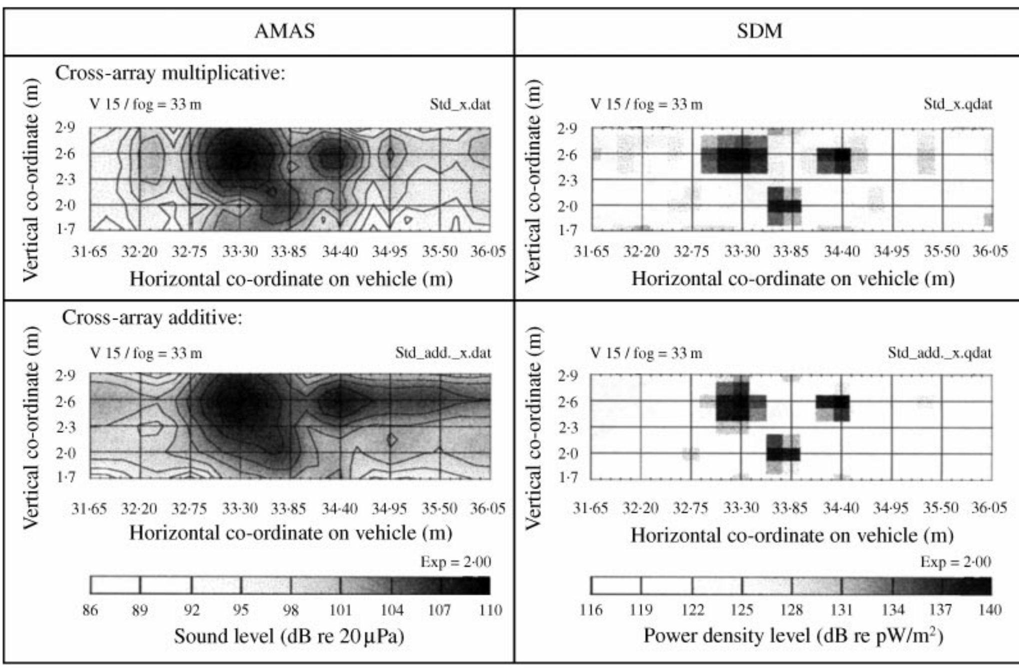

Figure 6. AMAS and SDM analysis of ICE-V with three mounted loudspeakers at 280 km/h. Upper row: multiplicative cross-array, lower row: additive cross-array.

distribution delivered by the SDM analysis. Preferably, *it may be larger for other applications*, *where the sources do not exhibit the single point characteristics of the present case*). In Figure 7 the difference between the SDM calculation and the single source values measured directly at rest is shown as a function of the pass-by co-ordinate of the train. The error is smallest in the region 33–34 m, which is the situation shown in Figure 6 (sources opposite to the array position). For other situations when the sources are approaching or leaving the array position the error increases but it does not exceed 3 dB. This effect is due to a directional characteristic of the loudspeakers which had been detected during the measurement

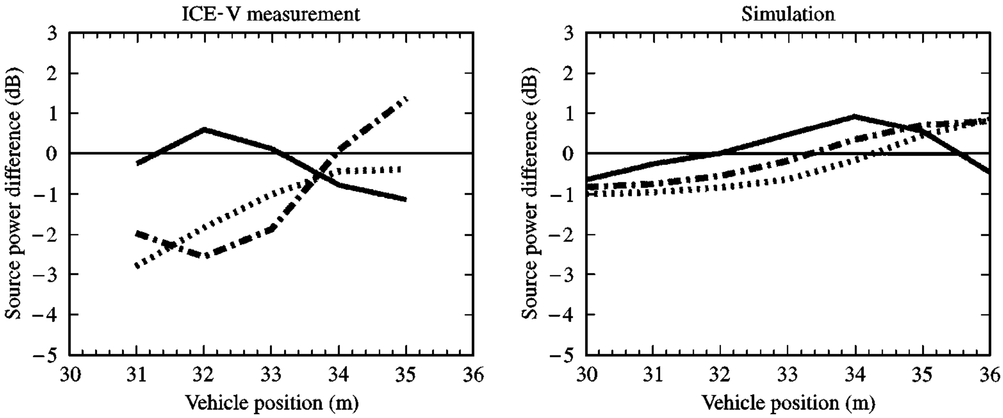

Figure 7. Error in source power level estimation for pass-by history. ▬, Q1 (585 Hz); ‐‐‐, Q2 (818 Hz); ┅, Q3 (992 Hz).

at rest. The equivalent result of a computer simulation for the same case but with a perfect omnidirectional behaviour of the sources is shown in Figure 7 as a comparison. The power estimate error now is $\leqslant 1$ dB. This remaining error cannot be avoided and is a general problem caused by the unstationary situation during pass-bys at high speeds, when the train moves a large distance within the time window which is necessary for the analysis (*AMAS uses the swept focus technique within one time window, but SDM is defined directly in the frequency domain and therefore cannot simulate changing effects which take place during this time interval*).

ACKNOWLEDGMENT

This work has been financed by the Deutsche Bahn AG within the frame of the research program DEUFRAKO, Annex K2.

REFERENCES

1. DeuFrako, Annex K. *Final Report*, December 1994.
2. S. Brühl and K.-P. Schmitz 1993 *Proceedings Internoise*, *Leuwen* 1311–1314. Noise source localization on highspeed trains using different array types.
3. S. Brühl 1997 *Technical Report IF 7M*11 *T*1.*DC* (*DeuFraKo*, *Annex K*2), Source density modelization of 2D array measurement data.
4. S. Brühl 1997 *Technical Report* 1*F* 7*G*18 *T*1.*DA* (*DeuFraKo*, *Annex K*2), Computer simulation of 2D source density modelization.
5. S. Brühl 1996 *Technical Report* 1*F* 6*S*19 *T*1.*DA* (*DeuFraKo*, *Annex K*2), Test program for SDM validation.
6. S. Brühl 1997 *Technical Report* 1*F* 7*D*15 *T*1.*DA* (*DeuFraKo*, *Annex K*2), 2D source density modelization of experimental test data. (to be approved).